

Hyperfine interactions of Sm and Co in $\text{Sm}_2\text{Co}_{17}$

E. Potenziani and D. I. Paul
Columbia University, New York, New York 10027

A. Tauber
U.S. Army Electronic Technology and Devices Laboratory, Fort Monmouth,
New Jersey 07703
(Received 26 March 1981)

DTIC
ELECTE
S APR 14 1983 D

AD A 126729

The Sm and Co hyperfine fields in $\text{Sm}_2\text{Co}_{17}$ have been measured at 4.2 K by means of the zero-field NMR spin-echo technique. The Sm resonance shows the existence of the $\text{Th}_2\text{Ni}_{17}$ -type structure with two inequivalent sites for the Sm nucleus having hyperfine fields of 3.40×10^6 and 3.48×10^6 G. It also shows that the effect of the mixing of the excited $J = \frac{7}{2}$ level into the ground $J = \frac{5}{2}$ multiplet by crystal- and exchange-field effects had a smaller effect on the hyperfine interaction than was expected. The hyperfine fields of the ^{59}Co resonance show a broad distribution from 110 to 220 MHz which we were able to correlate to the number of neighboring Co and Sm atoms surrounding the site in question.

INTRODUCTION

The compound $\text{Sm}_2\text{Co}_{17}$ is of considerable interest because of its own intrinsic magnetic characteristics such as a high-energy product and magnetocrystalline anisotropy as well as its potential commercial applications when alloyed with small amounts of other metals.¹⁻⁴

Among the trivalent rare-earth metal series, Sm^{3+} is interesting in that the energy separation between the ground $J = \frac{5}{2}$ and excited $J = \frac{7}{2}$ multiplets is only 1435 K. As such, the crystalline and exchange fields mix the higher multiplets into the ground state with the possibility of strongly affecting the hyperfine interactions.⁵ Quantitative analyses of the magnetization and magnetocrystalline anisotropy of $\text{Sm}_2\text{Co}_{17}$ have been extensively reported⁶ as have its crystallographic peculiarities.^{7,8}

We have performed zero-field spin-echo NMR on the ^{149}Sm , ^{147}Sm , and ^{59}Co nuclei in $\text{Sm}_2\text{Co}_{17}$ at 4.2 K. For the ^{149}Sm resonance we compare the experimentally obtained hyperfine field with that obtained from second-order perturbation theory, taking into account the mixing of the $J = \frac{7}{2}$ level into the $J = \frac{5}{2}$ level. The ^{59}Co resonance displays a broad six-peak distribution but we were able to correlate the resonant peaks to their respective sites with reasonable certainty.

EXPERIMENTAL

The intermetallic compound $\text{Sm}_2\text{Co}_{17}$ was obtained by induction melting stoichiometric amounts of 99.9% pure samarium and 99.99% pure cobalt in a boron nitride crucible under 12.6 kg/cm² of argon backpressure. Owing to the volatility of Sm metal this high backpressure, together with rapid melting, was required. The resultant weight loss was on the order of 0.2%. The 2:17 button was subsequently homogenized in an evacuated quartz vessel at 1180°C for four hours. After rapid quenching, the 2:17 button was ground under very dry toluene in a conventional ball milling apparatus. The resulting 2:17 slurry was vacuum dried and sifted to a 10–40 μm particle size. Subsequent x-ray diffraction analysis showed no trace of a second phase to within 5%.

The NMR sample consisted of about 15 g of this powder sealed in an epoxy binder and aligned in a magnetic field of several kilogauss while the epoxy was allowed to cure. The magnetic field mechanically aligns the particles along the easy *c* axis and gives us a strong domain-wall resonance when the rf is applied parallel to this alignment direction.

For the low-frequency ^{59}Co resonance (100–250 MHz), the equipment used was similar to that

DTIC FILE COPY

described by Streever and Uriano.⁹ The tuned coil was replaced by a rectangular cavity for the higher-frequency Sm work. Measurements were performed at 4.2 K using an exposed tip Dewar which fits into the resonant cavity. As such, the sample was physically immersed in liquid helium for all measurements.

The zero-field spin-echo NMR spectra were obtained by the conventional method of plotting echo amplitude versus frequency while keeping pulse width ($\sim 1-2 \mu\text{sec}$) and pulse separation ($10-40 \mu\text{sec}$) constant for each nucleus. The echo amplitudes were not corrected for the frequency dependence of the induced echo signal and nuclear polarization. This would give us a ν^2 dependence of the echo signal and, for a reasonable comparison of echo intensities, all observed echo amplitudes should be normalized by dividing each intensity by ν^2 at that point. The standard method of measuring echo intensities, that of comparing the echo to a calibrated rf pulse which passes through the same electronic amplification chain, eliminates to a great degree the effects of equipment frequency response on echo intensity measurements.

RESULTS

In Fig. 1 we have the Sm NMR resonance spectrum. The peaks around 502 MHz are from the ^{149}Sm resonance and the group of peaks centered at 603 MHz is due to the ^{147}Sm resonance. Interestingly enough, these are very close to the resonant frequencies found for SmCo_5 .¹⁰ The average line

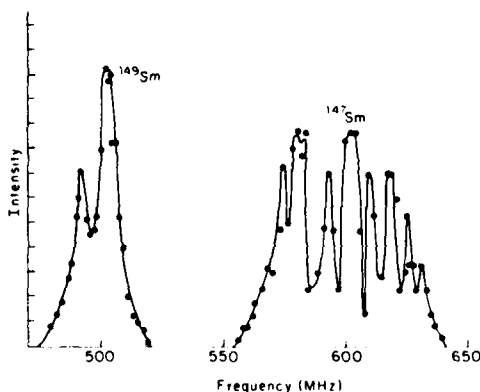


FIG. 1. ^{149}Sm and ^{147}Sm NMR spectrum of $\text{Sm}_2\text{Co}_{17}$ at 4.2 K. The echo amplitudes have not been corrected for the frequency dependence of the echo signal.

separation of the ^{147}Sm resonance yields a quadrupole interaction parameter $P(^{147}\text{Sm})$ of magnitude equal to $4.0 \pm 0.3 \text{ MHz}$, where

$$P = 3e^2qQ/4I(2I-1)\hbar. \quad (1)$$

NMR measurements were carried out on samples with the rf applied parallel and perpendicular to the alignment direction. The decrease in echo amplitude when the rf is perpendicular to the alignment direction confirms the presence of strong domain-wall excitation.

We note that the ^{149}Sm resonance is actually made up of two peaks at 491 and 502 MHz. Spin-lattice relaxation-time measurements were performed on both peaks using a sequence of $20-40 \mu\text{sec}$ rf pulses which was sufficient to thoroughly saturate our samples. The decay curve behaved exponentially, yielding T_1 's of 130 and 70 μsec for the 491- and 502-MHz peaks, respectively. Spin-spin relaxation-time measurements yielded nonexponential decay curves which approached a T_2 on the order of 200 μsec .

The ^{59}Co resonance (Fig. 2) extended from 105 to 225 MHz. We see a broad six-line pattern with peaks at 114, 133, 152, 163, 177, and 210 MHz. The experimental results are summarized in Table I and the assignment of the peaks to their respective sites is explained in the discussion.

DISCUSSION

Both Sm isotopes have $I = \frac{7}{2}$, but because of the large quadrupole moment of ^{147}Sm , $Q = -0.18b$,¹¹

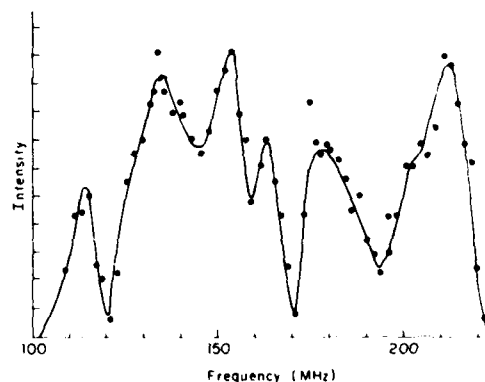


FIG. 2. ^{59}Co NMR spectrum of $\text{Sm}_2\text{Co}_{17}$ at 4.2 K. The echo amplitudes have not been corrected for the frequency dependence of the echo signal.

TABLE I. Summary of relaxation time and hyperfine-field data.

Nucleus	Site	Frequency (MHz)	$ H_{\text{eff}} $ (kG)	T_1 (μsec)	T_2 (μsec)
^{149}Sm	2c	491	3400 ± 20	130	200^a
	2b	502	3480 ± 20	70	200^a
^{59}Co		114	113 ± 3		260
	12k	133	132 ± 3		445
	6g	152	150 ± 3		120
	12j	163	161 ± 3		90
	4f	177	175 ± 3		270
		210	208 ± 3		170

^aThese relaxation times are approximate since the spin-echo decay envelope generally behaved nonexponentially.

versus the smaller moment of ^{149}Sm , $Q=0.058b$,¹² the quadrupole splitting is partially resolved into seven lines only for the ^{147}Sm resonance. The actual ^{147}Sm resonance consists of two overlapping seven-line spectra, as can be seen in Fig. 1.

In $\text{Sm}_2\text{Co}_{17}$ we can have the hexagonal TbCu_7 -type structure ($D_{6h}^1 P6/mmm$),⁷ the rhombohedral $\text{Th}_2\text{Zn}_{17}$ -type structure ($D_{3d}^5 R\bar{3}m$),⁷ and the hexagonal $\text{Th}_2\text{Ni}_{17}$ -type structure ($D_{6h}^4 P6_3/mmc$).^{7,13} X-ray diffraction analysis on our 2:17 powder yielded very diffuse lines due to the large amount of disorder present, but we were able to eliminate the possibility of our sample being of the $\text{Th}_2\text{Zn}_{17}$ -type structure due to the lack of the appropriate diffraction lines. The choice between the TbCu_7 and $\text{Th}_2\text{Ni}_{17}$ structures could not be made on the basis of x-ray analysis alone due to the similarity of their patterns. The TbCu_7 -type structure has only one site available for the Sm nucleus while the $\text{Th}_2\text{Ni}_{17}$ -type structure has two equally populated sites available. Although our spectrum for the ^{149}Sm resonance displays a double peak structure, there are several alternative explanations. The first possibility is that the two peaks arise from a TbCu_7 -type structure with a hyperfine-field anisotropy effect as described by Searle *et al.*¹⁴ If we take the ^{149}Sm nuclear magnetic moment as $-0.6631\mu_n$,¹⁵ we obtain hyperfine-field values for the 491- and 502-MHz peaks at $(3.40 \pm 0.02) \times 10^6$ and $(3.48 \pm 0.02) \times 10^6$ G, respectively. Following Searle's method the hyperfine-field anisotropy H_{HA} is given by

$$H_{\text{HA}} = \frac{2\eta\delta M_0}{\pi W\chi} \quad (2)$$

The enhancement factor η is estimated to be $\eta \approx 10 \times H_{\text{hyperfine}}/H_{\text{anisotropy}} \approx 200$,¹⁶ the domain-wall width $\delta \approx 30$ Å, the wall-to-wall spacing $W \approx 3000$ Å, and the saturation magnetization

$M_0 \approx 1000$ emu/cm³.¹⁷ Finally, the susceptibility χ is 6×10^{-3} emu/cm²Oe—obtained from a virgin hysteresis curve of a composition close to $\text{Sm}_2\text{Co}_{17}$.¹⁸ This gives us a $H_{\text{HA}} \approx 0.2 \times 10^6$ Oe while the actual linewidth of our ^{149}Sm resonance yields a H_{HA} of $(0.08 \pm 0.03) \times 10^6$ Oe. Such a result is in reasonable agreement considering the approximations that were used in the theory and data. However, the difference in the spin-lattice relaxation times of these two peaks, as noted in the section on results, lean heavily against this possibility. A second and more likely possibility is that the double peaks observed arise from the two inequivalent sites in a $\text{Th}_2\text{Ni}_{17}$ -type structure. The two sites available have very similar environments, except that (using Wyckoff notation) the 2c site does not have any axial Sm neighbors (Figs. 3 and 4). Because of this, the 2c site has a positive value for the crystal-field parameter A_2^0 , versus the negative value for the 2b site.¹⁹ Theoretically, this gives us, all other parameters remaining the same, a smaller hyperfine field for the 2c site. Also, this would imply a shorter spin-lattice relaxation time for the 2b site because of the greater number of

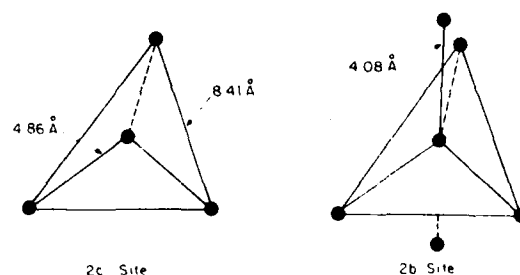


FIG. 3. The samarium ion together with its samarium nearest neighbors for $\text{Sm}_2\text{Co}_{17}$ with the $\text{Th}_2\text{Ni}_{17}$ ($D_{6h}^4 P6_3/mmc$) structure.

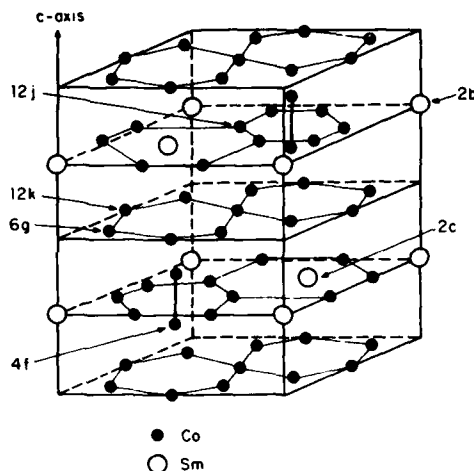


FIG. 4. Unit cell of the hexagonal $\text{Th}_2\text{Ni}_{17}$ -type structure.

neighboring Sm atoms. In accordance with these facts, we can therefore assume that the 491- and 502-MHz peaks correspond to the 2c and 2b sites, respectively.

We will now try to estimate the effects of crystal and exchange fields on the hyperfine field. The exchange field is taken along the hexagonal c axis, and we take for the crystal field parameters the same values as those given for the $\text{Th}_2\text{Zn}_{17}$ ($D_{3d}^5 R\bar{3}m$) structure—in as much as this is all that is currently available. These calculations would then be valid for the 6c rare-earth-metal site of the $\text{Th}_2\text{Zn}_{17}$ structure. We use the reasoning of Greedan and Rao¹⁹ and write

$$H = 2\mu_B S_z H_{\text{ex}} + B_2^0 O_2^0, \quad (3)$$

i.e., we ignore all the higher-order crystal-field terms which we know to be small.^{6,20} Following a previous example¹⁰ we will consider only the mixing of the ground $J = \frac{5}{2}$ state with the excited $J = \frac{7}{2}$ state and write the perturbed wave function as

$$\psi' = (1-a^2)^{1/2} \left| \frac{5}{2}, \frac{5}{2} \right\rangle + a \left| \frac{7}{2}, \frac{5}{2} \right\rangle \quad (4)$$

where we have used the notation of Ref. 21. The mixing parameter a is given by¹⁰

$$a = - \left[2\mu_B H_{\text{ex}} \left\langle \frac{7}{2} \middle| \Lambda \middle| \frac{5}{2} \right\rangle + (1-\sigma) A_2^0 \langle r^2 \rangle \frac{5}{2} \left\langle \frac{7}{2} \middle| \alpha \middle| \frac{5}{2} \right\rangle \right] \times \frac{\left[\left(\frac{7}{2} \right)^2 - \left(\frac{5}{2} \right)^2 \right]^{1/2}}{E_{7/2}^0 - E_{5/2}^0} \times \left[1 + \frac{\Delta_{5/2,5/2} - \Delta_{7/2,5/2}}{E_{7/2}^0 - E_{5/2}^0} \right]. \quad (5)$$

We take the values $\mu_B H_{\text{ex}} = 221 \text{ K}$,⁶ the shielding factor $(1-\sigma) \approx 0.5$, $A_2^0 \langle r^2 \rangle = -104 \text{ K}$,²² the energy difference between spin-orbit levels $(E_{7/2}^0 - E_{5/2}^0)/k_B = 1435 \text{ K}$, and the reduced matrix elements as $\langle \frac{7}{2} \middle| \Lambda \middle| \frac{5}{2} \rangle = 0.3912$ and $\langle \frac{7}{2} \middle| \alpha \middle| \frac{5}{2} \rangle = -0.1507$.²³

The energy splittings arising from the exchange and crystal fields are given by²¹

$$\Delta_{J,M} = 2\mu_B H_{\text{ex}} \frac{(g_J - 1)}{g_J} M \langle J \middle| \Lambda \middle| J \rangle + \langle J \middle| \alpha \middle| J \rangle (1-\sigma) A_2^0 \langle r^2 \rangle [3M^2 - J(J+1)] \quad (6)$$

or $(\Delta_{5/2,5/2} - \Delta_{7/2,5/2})/k_B = -722 \text{ K}$. This gives us a value for the mixing parameter of $a = -0.163$ and thus a value for the perturbed wave function ψ' . The hyperfine field is given by²⁴

$$H_{\text{eff}} = -2\mu_B \langle r^{-3} \rangle \langle \psi' | N_z | \psi' \rangle \quad (7a)$$

or

$$H_{\text{eff}} = H_{\text{eff}}(0) \left[1 - a^2 + 2a(1-a^2)^{1/2} \times (0.98) \frac{\langle \frac{7}{2} \middle| N \middle| \frac{5}{2} \rangle}{\langle \frac{5}{2} \middle| N \middle| \frac{5}{2} \rangle} + a^2 \frac{\langle \frac{7}{2} \middle| N \middle| \frac{7}{2} \rangle}{\langle \frac{5}{2} \middle| N \middle| \frac{5}{2} \rangle} \right] \quad (7b)$$

where $H_{\text{eff}}(0)$ is the "free-ion" hyperfine-field value²⁴ of $3.42 \times 10^6 \text{ G}$ obtained for the $J = \frac{5}{2}$, $M = \frac{5}{2}$ state and N_z is the hyperfine-field operator defined by

$$\langle J, M | N_z | J, M \rangle = \langle J \middle| N \middle| J \rangle \quad (7c)$$

and

$$\langle J+1, M | N_z | J, M \rangle = \langle J+1 \middle| N \middle| J \rangle \times [(J+1)^2 - M^2]^{1/2}.$$

This gives us $H_{\text{eff}} = 3.68 \times 10^6 \text{ G}$. We see that the expected hyperfine field should show an 8% increase above the free-ion value due to mixing of the excited $J = \frac{7}{2}$ level into the ground level. Since an increase of only 2% is observed for the 502-MHz peak, the discrepancy may be attributable to conduction-electron polarization, the influence of neighboring spins, or the approximations made in selecting the crystal-field terms.

For the case of the ^{59}Co resonance, Fig. 2, we have six distinct peaks. The $\text{Th}_2\text{Ni}_{17}$ -type struc-

TABLE II. ^{59}Co hyperfine-field data and parameters. Also listed are the calculated hyperfine fields according to Eq. (8).

Site	Frequency (MHz)	N_{Co}	N_{Sm}	$ H_{\text{eff}} $ (kG) expt.	$ H_{\text{eff}} $ (kG) calc.
4f	177	13	0	175	187
12j	163	11	2	161	161
6g	152	10	2	150	151
12k	133	9	3	132	137

ture has four inequivalent sites available to the Co atoms. In the case of other $R_2\text{Co}_{17}$ compounds,²⁵⁻²⁷ where R is a rare-earth atom, it was found that the hyperfine fields at the Co sites were not related to the moments of the surrounding Co atoms which vary from site to site but instead depended strongly on the nearest-neighbor Sm—Co and Co—Co distances. As such, we can fit these hyperfine fields to an expression of the form^{25,28}

$$H_{\text{eff}} = a\mu_{\text{Co}} + bN_{\text{Co}}\mu_{\text{Co}} + cN_{\text{Sm}}\mu_{\text{Sm}}, \quad (8)$$

where $\mu_{\text{Sm}} = 0.36\mu_B$, $\mu_{\text{Co}} = 1.64\mu_B$ and a , b , c are experimentally determined parameters. The first term is the hyperfine contribution due to the moment of the atom in question, the second term is the contribution from the neighboring Co atoms, and the third term is the contribution from the neighboring Sm atoms. The results are summarized in Table II. The best fit to the four peaks located at 133, 152, 163, and 177 MHz were obtained by using the values $a = -27.65 \text{ kG}/\mu_B$, $b = -6.65 \text{ kG}/\mu_B$, and $c = 5.49 \text{ kG}/\mu_B$. These values for a , b , and c yield reasonable agreement with the four experimental hyperfine fields. The peak at 210 MHz may be due to excess Co atoms that may result from the fast quenching,²⁹ i.e., nonequilibrium conditions, and from the volatility of Sm which may result in a Sm deficiency after melting. The peak at 210 MHz was observed even at 77 K while the four main peaks decreased into the noise at temperatures above 4.2 K. At present, the small peak at 114 MHz is still unexplained although it also shows the same basic intensity dependence on temperature as do the four main peaks. It may be due to the presence of a small amount of $\text{Sm}_2\text{Co}_{17}$ in the TbCu_7 -type structure.

CONCLUSION

The double-peaked structure displayed by the ^{149}Sm resonance confirms that our sample is of the

$\text{Th}_2\text{Ni}_{17}$ -type structure with two inequivalent rare-earth sites. The smaller hyperfine field of the 491-MHz peak, together with its longer relaxation time, enables us to assign this peak to the 2c site and the 502-MHz peak to the 2b site. The difference in heights, as shown in Fig. 1, may be attributable to the difference in the NMR domain-wall enhancement factor for the two sites. The most likely reason for the 2c site having almost the same hyperfine field as in the free-ion case is the absence of axial Sm neighbors. This is also consistent with its longer relaxation time. We note that the lower-than-theoretically calculated value for the hyperfine field of the 2b site (the 6c site of the $\text{Th}_2\text{Zn}_{17}$ -type structure) may be due to conduction-electron polarization effects or the mathematical approximations made in selecting the crystal-field terms.

The ^{59}Co resonance displays a well-resolved structure with the large peak at 210 MHz due, most likely, to a partial substitution of Co-Co pairs into rare-earth sites—possibly caused by a small Sm deficiency. The fact that we have been able to fit the ^{59}Co hyperfine fields to a three-parameter expression leads us to believe that the hyperfine field at each site depends only on nearest-neighbor distances rather than solely on the moment of the surrounding Co atoms.

ACKNOWLEDGMENTS

This work was supported in part by the U.S. Army Research Office, Grant No. DAAG-29-80-C0042. We particularly thank Dr. Fred Rothwarf for his continued help and encouragement and for his careful reading of our manuscript. We also thank the U.S. Army Electronics Technology and Devices Laboratory and Dr. R. L. Streever for the use of their facilities, and Mr. P. Kaplan for his help and encouragement.

- ¹K. J. Strnat, IEEE Trans. Magn. **MAG-8**, 511 (1972).
- ²K. S. V. L. Narasimhan and W. E. Wallace, in Proceedings of the Tenth Rare Earth Research Conference, Carefree, Arizona; *Magnetism and Magnetic Materials—1973 (Boston)*, Proceedings of the 19th Annual Conference on Magnetism and Magnetic Materials, edited by C. D. Graham and J. J. Rhyne (AIP, New York, 1974), p. 1248; J. Solid State Chem. **13**, 315 (1975).
- ³A. E. Ray and K. J. Strnat, IEEE Trans. Magn. **MAG-8**, 516 (1972).
- ⁴T. Ojima, S. Tomizawa, T. Yoneyama, and T. Hori, IEEE Trans. Magn. **MAG-13**, 1317 (1977).
- ⁵J. A. White and J. H. Van Vleck, Phys. Rev. Lett. **6**, 412 (1961); W. P. Wolf and J. H. Van Vleck, Phys. Rev. **118**, 1490 (1960).
- ⁶R. S. Perkins and S. Strüssler, Phys. Rev. B **15**, 477 (1977); **15**, 490 (1977).
- ⁷Y. Khan, Acta. Crystallogr. Sect. B **29**, 2502 (1973).
- ⁸Y. Kahn and B. Mueller, J. Less-Common Met. **32**, 39 (1973); Y. Kahn, *ibid.* **B30**, 861 (1974); K. H. J. Buschow, *ibid.* **11**, 204 (1966).
- ⁹R. L. Streever and G. A. Uriano, Phys. Rev. **139**, A135 (1965).
- ¹⁰R. L. Streever, Phys. Rev. B **12**, 4653 (1975).
- ¹¹G. H. Fuller, J. Phys. Chem. Ref. Data **5**, 835 (1976).
- ¹²G. H. Fuller and V. W. Cohen, Nucl. Data Tables **A5**, 433 (1969).
- ¹³G. Bouchet, J. Laforest, R. Lemaire, and J. Schweizer, C. R. Acad. Sci. **262**, 1 (1966).
- ¹⁴C. W. Searle, H. P. Kunkel, S. Kupca, and I. Martense, Phys. Rev. B **15**, 3305 (1977).
- ¹⁵I. Y. Chan and C. A. Hutchison, Jr., Phys. Rev. B **5**, 3387 (1972).
- ¹⁶M. P. Petrov, V. V. Moskalev, and G. A. Smolenskii, Zh. Eksp. Teor. Fiz. Pisma Red. **15**, 132 (1972); D. I. Paul, Phys. Rev. **131**, 178 (1963).
- ¹⁷R. L. Bergner, H. A. Leupold, J. T. Breslin, F. Rothwarf, and A. Tauber, J. Appl. Phys. **50**, 2349 (1979).
- ¹⁸H. Senno, Y. Tawara, and E. Hirota, Appl. Phys. Lett. **29**, 514 (1976).
- ¹⁹J. E. Greedan and V. U. S. Rao, J. Solid State Chem. **6**, 387 (1973).
- ²⁰S. G. Sankar, V. U. S. Rao, E. Segal, W. E. Wallace, W. G. D. Frederick, and H. J. Garrett, Phys. Rev. B **11**, 435 (1975).
- ²¹R. J. Elliott and K. W. H. Stevens, Proc. R. Soc. London Ser. A **219**, 387 (1953); S. Ofer, E. Segal, I. Nowik, E. R. Bauminger, L. Grodzins, A. J. Freeman, and M. Schieber, Phys. Rev. **137**, A627 (1965).
- ²²R. Rothwarf, H. A. Leupold, and A. Tauber, Bull. Am. Phys. Soc. **3**, 401 (1978).
- ²³R. J. Elliott and K. W. H. Stevens, Proc. R. Soc. London Ser. A **218**, 553 (1953).
- ²⁴B. Bleaney, in *Magnetic Properties of Rare Earth Metals*, edited by R. J. Elliot (Plenum, New York, 1972), Chap. 8.
- ²⁵R. L. Streever, in *Magnetism and Magnetic Materials*, Proceedings of the 20th Annual Conference on Magnetism and Magnetic Materials, edited by C. D. Graham, G. H. Lander, and J. J. Rhyne (AIP, New York, 1975), p. 462.
- ²⁶K. Inomata, T. Oshima, and T. Sawa, Fourth International Workshop on Rare Earth Cobalt Magnets and Their Applications, Hakone, Japan, 1979.
- ²⁷K. Inomata, Jpn. Appl. Phys. **15**, 821 (1976).
- ²⁸J. Itoh, K. Asayama, and S. Kobayshi, *Proceedings of the International Conference on Magnetism, Nottingham, 1964* (Institute of Physics and the Physical Society, London, 1964), p. 382.
- ²⁹J. B. A. A. Elemans, P. C. M. Gubbens, and K. H. J. Buschow, J. Less-Common Met. **44**, 51 (1976).

Accession For	
NTIS GRANT	<input checked="" type="checkbox"/>
DTIC TAB	<input type="checkbox"/>
Unannounced	<input type="checkbox"/>
Justification	
By	
Distribution/	
Availability Codes	
Dist	Avail and/or Special
A	21

